Universal properties of dipolar Bose polarons in two dimensions

J. Sánchez-Baena,[1] L. A. Peña Ardila,[2] G. E. Astrakharchik,[1] and F. Mazzanti[1]
[1]*Departament de Física, Campus Nord B4-B5, Universitat Politècnica de Catalunya, E-08034 Barcelona, Spain*
[2]*School of Science and Technology, Physics Divisio, University of Camerino, Via Madonna delle Carceri, 9B-62032 (MC), Italy*

(Received 11 April 2024; revised 3 July 2024; accepted 15 July 2024; published 15 August 2024)

We study the quasiparticle properties of a dipolar impurity immersed in a two-dimensional dipolar bath. We use the *ab initio* diffusion Monte Carlo technique to determine the polaron energy, effective mass, and quasiparticle residue. We find that both the polaron energy and quasiparticle residue follow a universal behavior with respect to the polarization angle when properly scaled in terms of the scattering length. This trend is maintained over a wide range of values of the gas parameter, even in the highly correlated regime. Instead, the effective mass shows growing anisotropy as the tilting angle is increased, which is induced, mainly, by the anisotropy of the impurity-boson dipole-dipole interaction. Surprisingly, the effective mass is larger in the direction of minimum interparticle repulsion. Finally, we use our Monte Carlo results to check the accuracy of perturbative approaches and determine their range of validity in terms of the gas parameter.

DOI: 10.1103/PhysRevA.110.023317

I. INTRODUCTION

Impurities interacting with a complex quantum-many-body environment have been the subject of intense research in recent years. In the solid-state realm, impurities interacting with an ionic crystal disrupt the media and are screened by lattice phonons, forming quasiparticles known as *polarons* [1]. Polarons have been found to play an important role in semiconductor transport [2], colossal magnetoresistance [3], as well as nonequilibrium phenomena such as quantum heat transport [4]. The high tunability and controllability of ultracold quantum gases offers an excellent platform to probe polaron physics in a clean environment, which has motivated a considerable amount of experimental [5–13] and theoretical [14–35] works. Polarons have been experimentally realized in bosonic [6–12] as well as fermionic [5,13] environments, and state-of-the art techniques like rf spectroscopy or the measurement of driven Rabi oscillations allow to probe quasiparticle properties like the polaron energy and the quasiparticle residue, respectively.

However, dipolar systems present rich physics due to the unique combination of traits of the dipole-dipole interaction (DDI): its anisotropy and long-range character in three dimensions. This mix gives rise to a wide variety of phenomena, such as the emergence of ultra-dilute self-bound droplets [36–41], supersolids [42–58] which may be even self-bound in the case of a dipolar mixture [59], striped liquids [60] and the anomalous emergence of supersolidity upon increasing temperature [61–63], among others. In the context of the polaron problem, an immediate question emerges: how do the unique properties of the DDI affect the quasiparticle properties and dynamics of an impurity immersed in a dipolar medium? Several theoretical works have addressed this question in a variety of different conditions: from nondipolar [24,27] and dipolar [29] impurities immersed in a dipolar fermionic medium, to an impurity-medium bilayer configuration [25,34] or dipolar [26,31,32] as well as nondipolar [28,33] impurities immersed in a dipolar Bose-Einstein condensate (BEC). It has also been shown that dipolar impurities can potentially function as tools to probe the properties of dipolar bosonic quantum droplets due to their neglectable back-action on the droplets [31]. In almost all cases, though, theoretical studies are restricted to an ultra-dilute bath, meaning that the characterization of the polaron properties for large gas parameters of the background is still a rather unexplored subject.

Precisely when the density (and thus, the correlations) of the medium are increased, and the interparticle distances become of the order of the range of interactions, it becomes relevant to determine the regime for which a universal description of the problem is quantitatively accurate. In ultra-dilute conditions where the impurity-medium interaction is short range, both the ground-state properties and the dynamics of the impurity are expected to be universal [10,11,14,19,23], that is, dependent only on the scattering length a and the density n. However, for impurity-bath interactions in the unitary limit [17,18] or for a sufficiently dense background [29,30], universality is expected to be lost at some point, where the description of the system becomes dependent on the details (range) of the interactions [30]. For instance, for the case of an impurity immersed on a Fermi gas in two dimensions, the universality in the polaron energy is lost for gas parameters as low as $x = 10^{-5}$, while the quasiparticle residue remains universal up to $x = 10^{-2}$ [29].

In this sense, the two-dimensional dipolar system in the absence of an impurity shows a universal behavior of its ground-state properties with respect to the polarization angle of the dipoles for surprisingly large values of the gas parameter [64]. That is, when dipoles are tilted with respect to the perpendicular direction of the plane and the DDI changes, the scaled energy $Ema^2/N\hbar^2$, scaled pair-distribution function $g(\vec{r}/a)$ and condensate fraction depend only on the gas parameter $x = na^2$. This is the case even in the ultra-correlated regime ($x \sim 100$). In this sense, this is a similar universality to

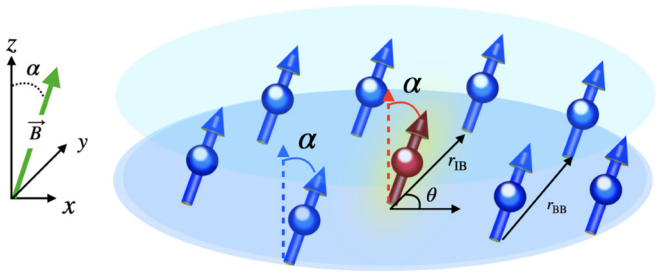

FIG. 1. Sketch of the system. Blue arrows depict dipolar atoms from the bath confined to the x-y plane and the red arrow shows the impurity. An external magnetic field is used to polarize all atoms and the impurity in the same direction, forming the tilting angle α with the respect to the direction normal to the plane. The azimuthal angle θ encodes the anisotropy of the system.

the one presented in Ref. [65] for a Rydberg impurity, where its absorption spectra for several Rydberg interactions (for different values of the principal quantum number) is the same as long as $x = na^3$ is kept constant.

In light of this unexpected universal behavior displayed by the bulk system, we address the question of whether this anomalous universality translates to the polaron properties once an impurity is introduced into the system. For that, we compute the quasiparticle properties (polaron energy, quasiparticle residue, and effective mass) of the repulsive Bose polaron as a function of the polarization angle of the dipoles for different values of the gas parameter of the bulk, reaching up to the very strongly correlated regime. We do so by means of the diffusion Monte Carlo (DMC) method. We set all particles (the impurity and the ones in the bath) polarized along the same direction in space. The dipolar interaction depends on the angle α formed by the polarization field and the z axis, and the dipolar strength C_{dd}. Denoting by I and B the impurity and a background atom, respectively, the dipolar interaction reads

$$V_{\sigma\sigma'}(\mathbf{r}_{ij}) = C_{dd}^{\sigma\sigma'}\left(\frac{1-3\sin^2\alpha\cos^2\theta_{ij}}{r_{ij}^3}\right), \tag{1}$$

where $\sigma, \sigma' \in \{I, B\}$. In this expression $\mathbf{r}_{ij} = \mathbf{r}_i - \mathbf{r}_j$ is the in-plane relative position vector between any pair of atoms, while $r_{ij} = |\mathbf{r}_i - \mathbf{r}_j|$ and θ_{ij} are the corresponding distance and relative orientation angle, respectively, as shown in Fig. 1. Furthermore, $C_{dd}^{\sigma\sigma'} = 6\pi\hbar^2\sqrt{d_\sigma d_{\sigma'}}/\mu^{\sigma\sigma'}$, with $d_\sigma = m_\sigma C_{dd}^{\sigma\sigma}/(12\pi\hbar^2)$ the corresponding dipolar length, and $\mu^{\sigma\sigma'} = m_\sigma m_{\sigma'}/(m_\sigma + m_{\sigma'})$ the reduced mass between two atoms. The expression in Eq. (1) shows that the dipolar interaction is anisotropic and depends on both the polarization angle α and the interaction strength C_{dd}, both of which determine the scattering length. The opposite is also true, namely, that a given a set of particles feel a different dipolar interaction when either α or the scattering length is changed.

II. SYSTEM AND NUMERICAL METHOD

The system consists of a single impurity interacting with a background of bosonic dipoles in two dimensions at fixed density n and at zero temperature, described by the Hamiltonian

$$\mathcal{H} = -\frac{\hbar^2}{2m_B}\sum_{i=1}^{N}\nabla_i^2 - \frac{\hbar^2}{2m_I}\nabla_I^2 + \sum_{i<j}V_{\mathrm{BB}}(\mathbf{r}_{ij}) + \sum_{i=1}^{N}V_{\mathrm{IB}}(\mathbf{r}_{iI}). \tag{2}$$

The first two terms in this expression represent the kinetic energy of the host bath and the impurity, while the last ones correspond to the dipolar interactions between the background atoms and with the impurity, respectively.

In the following we consider the impurity and background bosons to have the same mass, so we set $m_{\mathrm{I}} = m_{\mathrm{B}} = m$. This assumption is well suited, for example, when we consider the atoms in the bath and the impurity to be different isotopes of the same highly dipolar, heavy atom as could be ^{162}Dy and ^{164}Dy. This is also a realistic assumption when the impurity and the background particles correspond to the same isotopes, but in different hyperfine states. We also restrict the analysis to tilting angles $\alpha \in [0, 0.615]$ rad, as for larger values one has that $1 < 3\sin^2\alpha$, and thus the DDI ceases to be repulsive for all $\mathbf{r}_{ij}$, which induces a collapse into the system in the absence of additional hard core repulsive forces.

Within this model, the s-wave scattering length for both the $\{I, B\}$ and $\{B, B\}$ interaction pairs become [66]

$$a_{\sigma\sigma'}(\alpha, C_{dd}^{\sigma\sigma'}) \simeq \frac{mC_{dd}^{\sigma\sigma'}}{4\pi\hbar^2}\exp(2\gamma)\left(1-\frac{3\sin^2\alpha}{2}\right), \tag{3}$$

where γ is the Euler-Mascheroni constant $\gamma = 0.577\cdots$. These values fix another relevant parameter of the system, $\beta = C_{dd}^{\mathrm{IB}}/C_{dd}^{\mathrm{BB}} = a_{\mathrm{IB}}/a_{\mathrm{BB}}$, which sets the relative strength between the impurity-background and the background-background interactions. In this way, the system properties are governed by α, β, and the density n.

We perform the calculations using the diffusion Monte Carlo method [67]. In DMC, one numerically implements the imaginary time evolution equation

$$\psi_T(\mathbf{R})\psi(\mathbf{R}, \tau+\Delta\tau) = \int d\mathbf{R}' G(\mathbf{R}, \mathbf{R}', \Delta\tau)\frac{\psi_T(\mathbf{R})}{\psi_T(\mathbf{R}')}\psi_T(\mathbf{R}')\psi(\mathbf{R}', \tau), \tag{4}$$

where $\tau = it/\hbar$ is the imaginary time, $G(\mathbf{R}, \mathbf{R}', \Delta\tau) = \langle\mathbf{R}|\exp(-\hat{H}\Delta\tau)|\mathbf{R}'\rangle$ is the imaginary time Green's function, and $\psi_T(\mathbf{R})$ is the trial wave function, an input to the method. This trial wave function helps reduce the variance of the estimations if chosen appropriately. To numerically implement Eq. (4), one first obtains a statistical representation of the density associated to a given trial wave function, $\rho_T(\mathbf{R}) = |\psi_T(\mathbf{R})|^2$. This representation consists of a set of points in coordinate space named *walkers* (i.e., $\{\vec{R}\}_i = \{\vec{r}_1, \ldots, \vec{r}_N\}_i$ where i is the walker index). A set of transformations are then applied to the walkers, such that, at the end of the process, they statistically represent the probability distribution $\psi_0(\mathbf{R})\psi_T(\mathbf{R})$, with $\psi_0(\mathbf{R})$ the ground-state wave function of the system. These transformations are obtained by interpreting the quantity $G(\mathbf{R}, \mathbf{R}', \Delta\tau)\frac{\psi_T(\mathbf{R})}{\psi_T(\mathbf{R}')}$ as a probability distribution. Observables are estimated as

$$\langle\hat{O}\rangle = \frac{\int d\mathbf{R}\,\psi_T(\mathbf{R})\hat{O}\psi_0(\mathbf{R})}{\int d\mathbf{R}\,\psi_T(\mathbf{R})\psi_0(\mathbf{R})}. \tag{5}$$

Notice that any quantity that commutes with the Hamiltonian, such as the energy, can be computed exactly (up to statistical uncertainty) regardless of the choice of the trial wave function. We use a trial wave function of the Jastrow form

$$\psi_T(\mathbf{R}) = \prod_{i=1}^{N} f_{\mathrm{IB}}(\mathbf{r}_{il}) \prod_{i<j} f_{\mathrm{BB}}(\mathbf{r}_{ij}), \tag{6}$$

where the two-body correlation factors f_{IB} (impurity-background) and f_{BB} (background-background) are obtained from the solution of the zero-energy two-body problem, as done in previous works [64,66]. These functions have been matched with suitable large-distance phononic tails to recover the proper behavior of the many-body wave function.

III. RESULTS

In the following, we study how the polaronic properties (polaron energy, quasiparticle residue, and effective mass) and the pair-correlation function depend on the density n and the tilting angle of the dipoles α for a fixed ratio β. The dependence on β is reported for the polaron energy.

A. Polaron energy and pair-distribution function

The driving quantity in any DMC calculation is the ground-state energy, which therefore becomes in a natural way the first property to analyze. For a dilute system, the mean-field prediction for the polaron energy [21]

$$E_p^{(0)} = -\frac{4\pi n\hbar^2}{m \ln\left(n a_{\mathrm{IB}}^2\right)}, \tag{7}$$

is expected to hold, irrespective of the details of the interaction. In the present case, a_{IB} and a_{BB} present the same dependence on the polarization angle, according to Eq. (3). Consequently, for fixed impurity and bath, the ratio $a_{\mathrm{IB}}/a_{\mathrm{BB}} = \beta$ remains constant when α changes, and the product $E_p^{(0)}(\alpha) a_{\mathrm{BB}}^2(\alpha)$ becomes a function of the gas parameter $x = n a_{\mathrm{BB}}^2$ alone. This means that changing the polarization angle α leaves the mean-field polaron energy unchanged if the density is changed accordingly to keep the gas parameter constant.

Considering this property emerges from Eq. (7), it is, in principle, expected to hold only at low x. However, and surprisingly, it is still present up to very large values of the gas parameter $x \sim 100$, as shown in Fig. 2. We show in the figure the DMC results for the polaron energy, expressed in scattering length units, i.e., $E_p(\alpha)/[\hbar^2/m a_{\mathrm{BB}}^2(\alpha)]$, as a function of the tilting angle for three different values of the gas parameter ($x = 0.001$, 1, 10) and a fixed ratio $\beta = a_{\mathrm{IB}}/a_{\mathrm{BB}} = 10$. These parameters place our system away from the perturbative regime, meaning that the background gas of bosons is highly correlated and the impurity-bath interaction cannot be considered a perturbation. From the results, we see that the quantity $E_p(\alpha)/[\hbar^2/m a_{\mathrm{BB}}^2(\alpha)]$ is kept constant (except for small variations of less than 5%) when α changes for a fixed gas parameter. Thus, in a very good approximation, given a fixed value of β, the polaron energy is a function of the density n and the boson-boson a_{BB} (or impurity-boson a_{IB}) scattering length alone for different tilting angles, meaning that

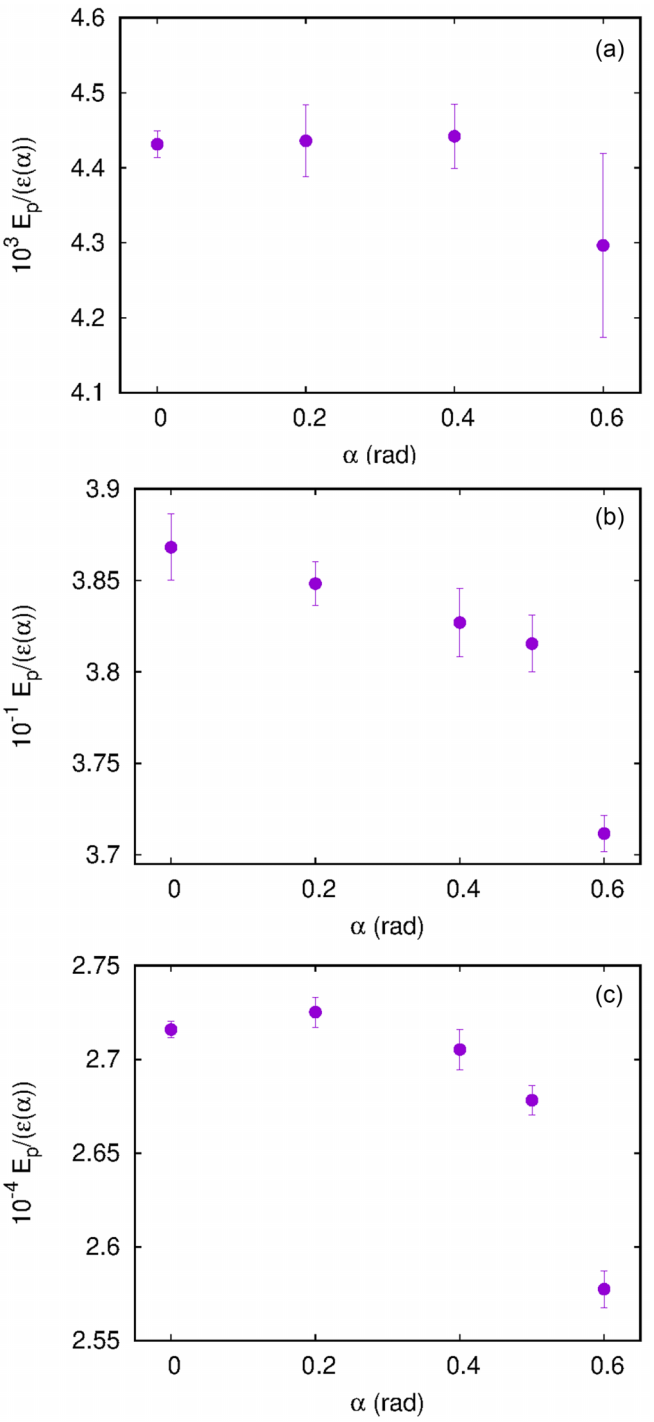

FIG. 2. DMC results for the polaron energy in scattering length units [i.e., $\epsilon(\alpha) = \hbar^2/m a_{\mathrm{BB}}^2(\alpha)$, with $a_{\mathrm{BB}}(\alpha)$ defined in Eq. (3)] for (a) $x = 0.001$, (b) $x = 1$, and (c) $x = 100$.

different dipolar interactions with different tilting angles display universality. The deviations from a constant of the rescaled polaron energy $E_p(\alpha)/[\hbar^2/m a_{\mathrm{BB}}^2(\alpha)]$ grow with α for the highest tilting angles considered, which indicates that universality starts to slightly break down in the limit $\alpha \to 0.615$ rad, whence the DDI acquires a negative contribution that induces a collapse into the system. This can be understood as follows: increasing α while keeping the gas parameter

constant implies progressively reducing the s-wave scattering length while increasing the density, which, in turn, decreases the interparticle distance and thus enhances finite range effects. These results align with the previous findings for the bulk system, where a similar universal behavior is observed [64]. In this sense, the universality present in this work is very much akin to the one discussed in Ref. [65], where it is shown that the absorption spectra of a Rydberg atom is a function solely of the parameter na^3, despite the Rydberg potential depending on the principal quantum number, which controls its depth and its range. This means that all Rydberg interactions show the same universal response which only depends on n and a, in much the same way that different dipole-dipole interactions with different tilting angles display results that only depend on n and $a_{\rm BB}$, given that β is kept fixed.

Given this trend displayed by the polaron energy and the analytic expression of the scattering length in Eq. (3), the dipolar polaron energy can be considered to be a function of β, n, and $a_{\rm BB}$ alone that can be obtained from a fit to the corresponding Monte Carlo data. We obtained these fits for $\alpha = 0$ and two relevant values of the coupling strength: $\beta = 1.42$, corresponding to the case of a Dy impurity immersed in an Er bath, and the extreme case of a strongly interacting impurity $\beta = 10$. We checked that the polaron energy follows a law of the form

$$E_p(\alpha = 0) = \exp\{a[\ln(x) + c]^d + b\}\,\epsilon_d, \tag{8}$$

with $a = 0.94(8)$, $b = -16.30(1)$ for $\beta = 1.42$ and $a = 0.97(4)$, $b = -15.79(4)$ for $\beta = 10$. In both cases, $c = 11.99(3)$ and $d = 1.09(3)$. Also, $x = na_{\rm BB}^2$ and $\epsilon_d = \hbar^2/md_B^2$, where $d_{\rm B} = m_{\rm B}C_{dd}^{\rm BB}/(12\pi\hbar^2)$ is the dipolar length of the atoms of the bath. The energy for any other tilting angle can approximately be obtained by the relation

$$E_p(\alpha) \simeq E_p(\alpha = 0)\frac{\hbar^2/ma_{\rm BB}^2(\alpha)}{\hbar^2/ma_{\rm BB}^2(\alpha = 0)}. \tag{9}$$

The functional form of Eq. (8) is phenomenological, in the sense that it has not been derived from any first principles, but rather has been chosen such that the DMC results for $\alpha = 0$ can be reproduced with a small error. In all cases this error is slightly less than 10%.

A relevant question related to the previous results is the extent to which a perturbative approximation accurately describes the ground-state energy of the system for the dipolar polaron. In a perturbative scheme, the bath is usually described by a Bogoliubov Hamiltonian in the absence of the impurity, while the impurity-bath interaction is considered to be the (weak) perturbation. For the two-dimensional dipolar system considered in this work, the boson-boson and impurity-boson interactions in momentum space are taken to be described by the pseudopotentials [54]

$$V_{\sigma\sigma'}^{(p)}(\mathbf{k}) = -\frac{4\pi\hbar^2}{m\ln\left(na_{\sigma\sigma'}^2\right)} + \frac{C_{dd}^{\sigma\sigma'}k\pi\,\sin^2\alpha\cos 2\theta_k}{2}, \tag{10}$$

with θ_k the polar angle of the momentum vector. This pseudopotential is built such that its s-wave and d-wave scattering properties computed under the first-order Born approximation match those of the full dipole-dipole interaction, i.e., Eq. (1).

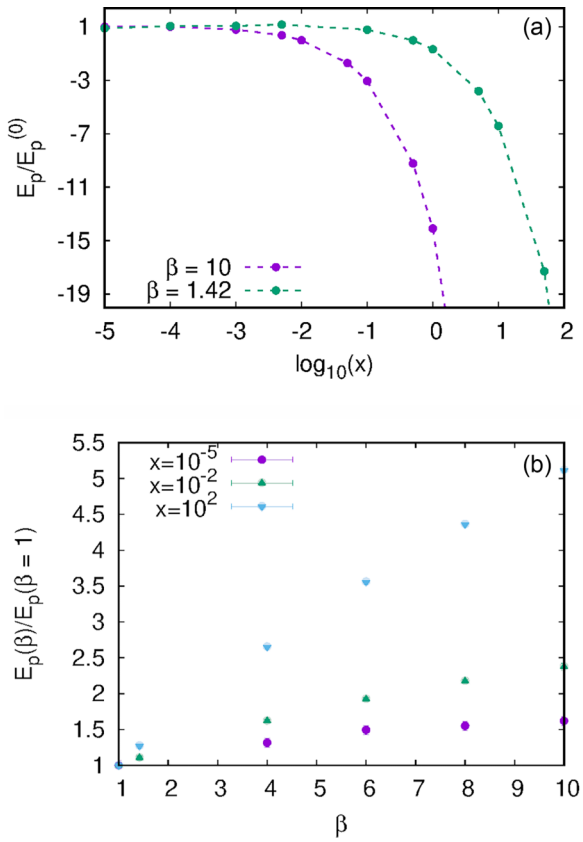

FIG. 3. (a) Ratio between the DMC (E_p) and the first-order perturbation theory [$E_p^{(0)}$, see Eq. (7)] polaron energies for $\beta = 1.42$ and $\beta = 10$. (b) Polaron energy as a function of the impurity-boson coupling $\beta = C_{dd}^{\rm IB}/C_{dd}^{\rm BB}$ (dimensionless) for different values of the gas parameter. Energies are rescaled with respect to its corresponding value at $\beta = 1$.

Note also that this pseudopotential incorporates finite-range effects via the anisotropic contribution in the second term. Within perturbation theory and using the Fröhlich Hamiltonian, one considers only processes where the impurity couples to a single excitation of the medium at once. To quantify the accuracy of the perturbative approach, we show in Fig. 3(a) the ratio of the DMC energies to the lowest-order perturbation prediction $E_p^{(0)}$ of Eq. (7). As it can be seen from the figure and as expected, the perturbative approximation holds only in the dilute limit, corresponding to gas parameter values $x \lesssim 0.01$ for $\beta = 1.42$ and $x \lesssim 0.001$ for $\beta = 10$. For larger values of x, higher-order effects, neglected in the lowest-order perturbative scheme, start to become important.

Finally, Fig. 3(b) shows the dependence of the polaron energy on the coupling ratio β for $\alpha = 0$ and several values of the gas parameter. Energies have been rescaled with respect to their values at $\beta = 1$ for the sake of comparison, which correspond to $E_p(x = 10^{-5}) = 1.25 \times 10^{-7}\epsilon_d$, $E_p(x = 10^{-2}) = 3.92 \times 10^{-4}\epsilon_d$ and $E_p(x = 10^2) = 58.18\epsilon_d$. We find that the relative variation of the polaron energy grows with increasing gas parameter. This is a consequence of the fully repulsive character of the dipole-dipole interaction and the fact that, for a fixed polarization angle, increasing the value of the gas parameter is equivalent to increasing the density of atoms of

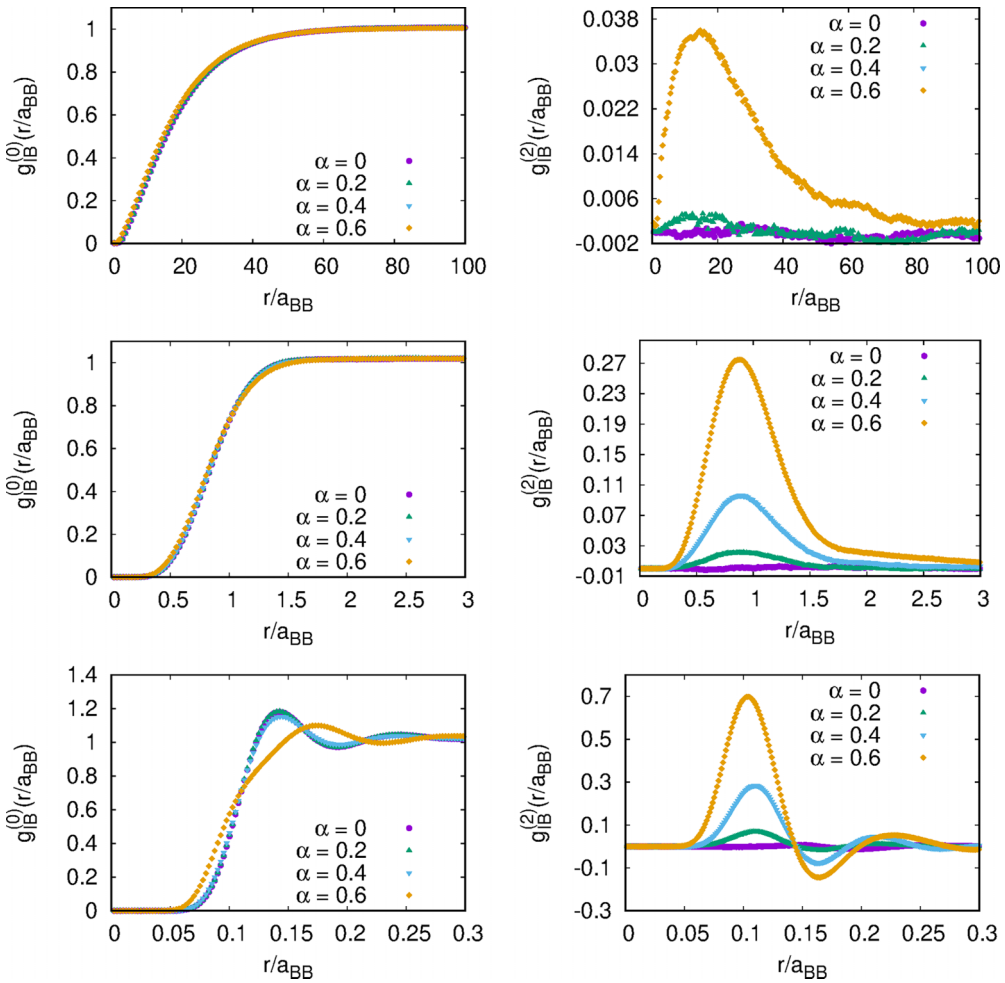

FIG. 4. s and d partial wave modes of the impurity-boson pair-distribution function (dimensionless) for three characteristic values of the gas parameter: $x = 0.001$ (top row), $x = 1$ (middle row), $x = 100$ (bottom row). The impurity strength ratio is fixed to $\beta = 10$. The tilting α is expressed in radians.

the bath. We show only the variation of the polaron energy with respect to β at zero tilting angle because the energy for any other value of α can be obtained through Eq. (9) due to the universality of the results with respect to the tilting angle.

Additional insight into the dipolar polaron universality can be drawn from the relation between the polaron energy and the boson-boson and impurity-boson pair distribution functions. These quantities are defined as

$$g_{BB}(\mathbf{r_1} - \mathbf{r_2}) = \frac{N(N-1)}{n^2} \frac{\int d\mathbf{r_3} \cdots d\mathbf{r_N} d\mathbf{r_I} |\Psi(\mathbf{R})|^2}{\int d\mathbf{R} |\Psi(\mathbf{R})|^2}, \quad (11)$$

$$g_{IB}(\mathbf{r_I} - \mathbf{r_1}) = \frac{N}{n_I n} \frac{\int d\mathbf{r_2} \cdots d\mathbf{r_N} |\Psi(\mathbf{R})|^2}{\int d\mathbf{R} |\Psi(\mathbf{R})|^2}, \quad (12)$$

with $\mathbf{R}$ representing the set of all particle coordinates, $n = N/V$ and $n_I = 1/V$ being the average bath and impurity density, respectively. Actually, these two functions can be expanded in partial waves and, due to the anisotropy of the dipolar interaction, they present nonzero contributions beyond the s-wave. We show in Fig. 4 the first two modes of

$$g_{IB}(\mathbf{r_I} - \mathbf{r_1}) = \sum_{l=0}^{\infty} g^{(2l)}_{IB}(r) \cos 2l\theta, \quad (13)$$

for $\beta = 10$ and different gas parameters and tilting angles. Results for $g_{BB}(\mathbf{r_1} - \mathbf{r_2})$ are very similar to those obtained for the dipolar bulk case in Ref. [64]. As it can be seen from the figure, the isotropic mode is universal with respect to the tilting angle up to $\alpha \simeq 0.4$ since all curves collapse to a single one when plotted in terms of the rescaled distance r/a_{BB}. This happens even for abnormally large values of the gas parameter. However, the first anisotropic mode does not show any universality in α at all. However, we also see that, up to $\alpha \simeq 0.4$, the isotropic mode clearly dominates over the anisotropic contribution unless both α and x are large, leading to an essentially universal behavior, similarly to what it was reported in Ref. [64] for the bulk. The pair distribution functions is related to the potential energy of the system by the relation

$$\langle V \rangle = n \int d\mathbf{r} V_{IB}(\mathbf{r}) g_{IB}(\mathbf{r}) + \frac{nN}{2} \int d\mathbf{r} V_{BB}(\mathbf{r}) g_{BB}(\mathbf{r}), \quad (14)$$

where the first term comes from the interaction between the impurity and the rest of the particles in the medium, while the second term accounts for the contribution of the bath. From this expression, one can recover the total energy of the system

through the Hellmann-Feynman theorem [64,68]

$$E = \int_0^1 du \Big\{ n \int d\mathbf{r} V_{\mathrm{IB}}(\mathbf{r}) g_{\mathrm{IB}}(\mathbf{r}, u) + \frac{nN}{2} \int d\mathbf{r} V_{\mathrm{BB}}(\mathbf{r}) g_{\mathrm{BB}}(\mathbf{r}, u) \Big\}, \tag{15}$$

where $g_{\mathrm{IB}}(\mathbf{r}, u)$ and $g_{\mathrm{BB}}(\mathbf{r}, u)$ stand the pair distribution functions corresponding to the Hamiltonian $\hat{H} = \hat{H}_{\mathrm{kin}} + \hat{H}_{\mathrm{pot}} u$, with $\hat{H}_{\mathrm{kin}}$ and $\hat{H}_{\mathrm{pot}}$ the kinetic and potential terms of the Hamiltonian in Eq. (2), respectively. The polaron energy can then be recovered from the energy difference

$$\begin{aligned} E_p &= E(N, 1) - E(N, 0) \\ &= \int_0^1 du \Big\{ n \int d\mathbf{r} V_{\mathrm{IB}}(\mathbf{r}) g_{\mathrm{IB}}(\mathbf{r}, u) \\ &\quad + \frac{nN}{2} \int d\mathbf{r} V_{\mathrm{BB}}(\mathbf{r}) g_{\mathrm{BB}}(\mathbf{r}, u) \Big\} \\ &\quad - \frac{nN}{2} \int d\mathbf{r} V_{\mathrm{BB}}(\mathbf{r}) \tilde{g}_{\mathrm{BB}}(\mathbf{r}, u), \end{aligned} \tag{16}$$

where $E(N_B, N_I)$ denotes the ground-state energy of a system with N_B bosons and N_I impurities, and $\tilde{g}_{\mathrm{BB}}(\mathbf{r}, u)$ is the boson-boson pair distribution function of the bulk system (i.e., for absent impurity). In this way, the universality in the polaron energy can be understood as being inherited from the corresponding behavior of the pair distribution functions.

B. Quasiparticle residue

Another experimentally relevant quantity in the study of the polaron physics is the quasiparticle residue Z, which quantifies the overlap between the full wave function of the system and a state conformed by a noninteracting impurity and a vacuum of excitations. A mixed estimator for this quantity can be obtained in DMC from the long-range asymptotic behavior of the one-body density matrix associated to the impurity [21,69]

$$Z = \lim_{r\to\infty} \rho(\mathbf{r}) = \lim_{r\to\infty} \left\langle \frac{\psi_T(\mathbf{r}_1 + \mathbf{r}, \mathbf{r}_1, \cdots, \mathbf{r}_N)}{\psi_T(\mathbf{r}_1, \mathbf{r}_1, \cdots, \mathbf{r}_N)} \right\rangle, \tag{17}$$

where ψ_T is the many-body trial wave function guiding the simulation. We report in Fig. 6(a) the dependence of Z on the polarization angle α for different values of the gas parameter and $\beta = 10$. As can be seen, Z is also independent of α and seems to depend on the gas parameter exclusively, even for the largest values of x where interatomic correlations play an important role. In other words, the quasiparticle residue shows a clear universal behavior with respect to the tilting angle. This surprising property can be hinted already at the perturbative level using the simple model described above. To second order and using the interaction in Eq. (10) one finds

$$Z^{(2)} = \left(1 + \frac{n}{(2\pi)^2} \int d\mathbf{k} \left(V_{\mathrm{IB}}^{(p)}(\mathbf{k}) \right)^2 \frac{\epsilon_{\mathbf{k}}}{E(\mathbf{k})} \frac{1}{(\epsilon_{\mathbf{k}} - E(\mathbf{k}))^2} \right)^{-1}, \tag{18}$$

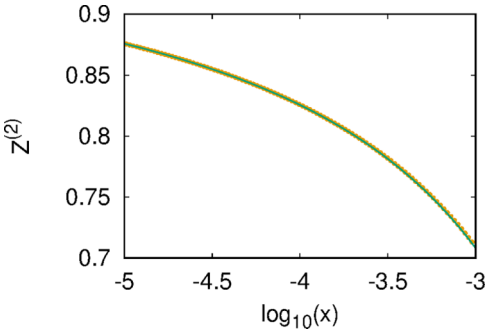

FIG. 5. Second-order perturbation theory results for the quasiparticle residue Z (dimensionless) for a bath with (orange dots) and without (green solid line) the finite range, anisotropic contribution of the boson-boson interactions [see Eq. (10)]. In both cases, $\alpha = 0.6$ rad for the impurity-boson interaction.

with $\epsilon_{\mathbf{k}} = \frac{\hbar^2 k^2}{2m}$ and $E(\mathbf{k}) = \sqrt{\epsilon_{\mathbf{k}}(\epsilon_{\mathbf{k}} + 2nV_{\mathrm{BB}}^{(p)}(\mathbf{k}))}$ the excitation spectrum of the bulk. Interestingly, getting rid of the anisotropic contribution to the bath-bath pseudopotential [second term on the rhs of Eq. (10)] that enters Z through the excitation spectrum of the medium leaves the quasiparticle residue essentially unchanged. This is shown in Fig. 5, where we compare the values of Z obtained with and without this contribution for different values of the gas parameter and $\alpha = 0.6$. In this way, the only relevant anisotropic contribution to Z comes from the impurity-bath interaction. However, the lowest-order anisotropic contribution is proportional to $\sin^4\alpha \ll 1$ since the term proportional to $\sin^2\alpha \cos 2\theta_k$ coming from $[V_{\mathrm{IB}}^{(p)}(\mathbf{k})]^2$ yields zero contribution when the angular integration is evaluated. This means that, at the perturbative level, the dependence of Z on the density and the impurity-bath scattering length is the same as that of an isotropic system with zero range interactions, and thus Z is a function of the gas parameter alone [21].

At this point, one can also compare the DMC prediction of the quasiparticle residue to the results obtained with perturbation theory, as a way to benchmark the perturbative approach. We show in Fig. 6(b) the DMC estimation of Z together with the perturbative result obtained from Eq. (17) for the two cases $\beta = 1.42$ and $\beta = 10$ and $\alpha = 0$. Because of universality with respect to the polarization angle, the same results hold for any other value of α. As it can be seen, the predictive power of the perturbative approach worsens with increasing x and/or β, as happens with the polaron energy. In this case, though, the situation is worse as the perturbative prediction ceases to reproduce the DMC data at lower gas parameter values, at least for $\beta = 10$. Remarkably, for the lowest coupling case, the regime where Z is close to unity extends up to $x \lesssim 10^{-2}$.

C. Effective mass

The last quantity we address in this work is the polaron's effective mass. To obtain the effective mass in DMC, one can track the diffusion movement of the polaron in imaginary time. This is done by calculating its mean-square displacement according to the expression

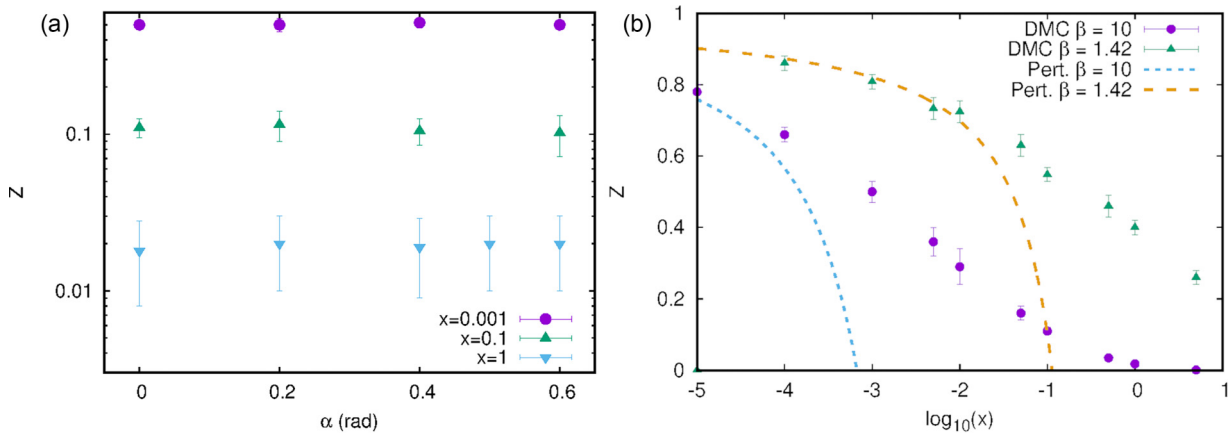

FIG. 6. (a) DMC results for the quasiparticle residue (dimensionless) as a function of the tilting angle for several values of the gas parameter for $\beta = 10$. (b) DMC results (dots) and perturbative results (solid lines) for Z obtained for $\alpha = 0$ rad as a function of the gas parameter.

$\frac{m}{m^*} = \lim_{\tau\to\infty} \frac{\langle|\Delta \mathbf{r}_I(\tau)|^2\rangle}{4D\tau}$ [21,29]; with $D = \hbar^2/(2m)$ the diffusion constant of a free particle, and $\langle|\Delta \mathbf{r}_I(\tau)|^2\rangle = \langle|\mathbf{r}_I(\tau) - \mathbf{r}_I(0)|^2\rangle$, $\tau = it/\hbar$ being the imaginary time of the simulation. Due to the anisotropic character of the dipolar interaction, the effective mass turns out to depend on the impurity's momentum direction for $\alpha \neq 0$. To quantify this effect, one can define an anisotropic effective mass by tracking the position of the impurity in each direction separately, according to $\frac{m}{m^*_\chi} = \lim_{\tau\to\infty} \frac{\langle|\Delta \chi_I(\tau)|^2\rangle}{2D\tau}$ with $\chi = x$ or y. Notice that the previous expression contain a factor of 2 instead of 4 in the denominator, as in this case the diffusion is treated as one-dimensional.

In any case and as done before, it is interesting to discuss first the predictions of perturbation theory. To second order, the effective mass is obtained from the second-order polaron energy [32]

$$E_p^{(2)} = \frac{\langle \mathbf{P}, 0|\hat{H}_{\rm IB}|\Psi_1\rangle}{\langle\Psi||\Psi\rangle}, \tag{19}$$

where $\langle \mathbf{P}, 0|$ denotes a state with a non-interacting impurity with momentum $\mathbf{P}$ and a zero-momentum medium. In much the same way, $|\Psi\rangle = |\mathbf{P}, 0\rangle + \lambda|\Psi_1\rangle$ with λ a perturbative parameter proportional to the strength of the impurity-medium interaction and $|\Psi_1\rangle$ the first-order contribution to the total wave function accounting for the perturbation.

Evaluating Eq. (19) and performing a Taylor expansion in terms of the impurity momentum, the P^2 contribution results in the following momentum-dependent correction to the polaron energy

$$\Delta E = -\frac{P^2}{2m}\frac{1}{(2\pi)^2}\int d\mathbf{k}\, n\big(V_{\rm IB}^{(p)}(\mathbf{k})\big)^2 \frac{\epsilon_{\mathbf{k}}}{E_{\mathbf{k}}}\frac{2\hbar^2k^2}{(\epsilon_{\mathbf{k}}+E_{\mathbf{k}})^3}\cos^2\theta, \tag{20}$$

where θ is the angle between the impurity momentum $\mathbf{P}$ and the integration momentum $\hbar\mathbf{k}$, which forms an angle ϕ with the x axis. The effective mass is then obtained from the momentum-dependent part of the polaron energy, which is given by the sum of impurity kinetic energy and the correction in Eq. (20), i.e.,

$$\begin{aligned}\frac{P^2}{2m^*} &= \frac{P^2}{2m} + \Delta E = \frac{P^2}{2m}\left(1 + \frac{2m\Delta E}{P^2}\right)\\ &= \frac{P^2}{2m}\left(1 - \frac{1}{(2\pi)^2}\int d\mathbf{k}\, n\big(V_{\rm IB}^{(p)}(\mathbf{k})\big)^2\right.\\ &\quad\left.\times\frac{\epsilon_{\mathbf{k}}}{E_{\mathbf{k}}}\frac{2\hbar^2k^2}{(\epsilon_{\mathbf{k}}+E_{\mathbf{k}})^3}\cos^2\theta\right).\end{aligned} \tag{21}$$

This result indicates that the inclusion of the second term in the pseudopotential of Eq. (10) leads to an anisotropic effective mass, induced by the angular dependence on the impurity's momentum vector. In particular, for an impurity moving along the x axis, m^* is replaced by m^*_x in Eq. (21), and this results into the substitution $\cos^2\theta \to \cos^2\phi$ while for a impurity moving along the y axis, computing m^*_y implies setting $\cos^2\theta \to \sin^2\phi$. Furthermore and as happens with the quasiparticle residue, the anisotropy of the boson-boson interactions that enters Eq. (21) through the excitation spectrum of the background has little impact on m^* compared to the impurity-boson potential. Since, as usual, the second-order correction to the polaron energy is negative, $m^* > m$, and the impurity acts as a heavier quasiparticle in the medium.

Figure 7 shows the ratios m/m^*_x and m/m^*_y obtained with second-order perturbation theory for $\beta = 1.42$ and $\alpha = 0.6$ as a function of the gas parameter. As one can see, the effective mass is larger when the polaron moves along the x axis. This is because the anisotropy in the effective mass is determined by the anisotropy of the impurity-bath interaction in momentum space, which is maximally repulsive along this direction. The corresponding DMC predictions for the effective mass in the x (or y) axis are also shown in the plot. Because the noise in the estimation in the effective mass is large, it prevents a clear observation of its anisotropic character but at large-enough gas parameters and impurity-bath coupling strengths. This implies that, in this regime, the DMC results for the effective mass along the x and y axes are indistinguishable up to statistical noise, which is why only a set of points is shown. This is an issue even when long simulations, which accumulate a large

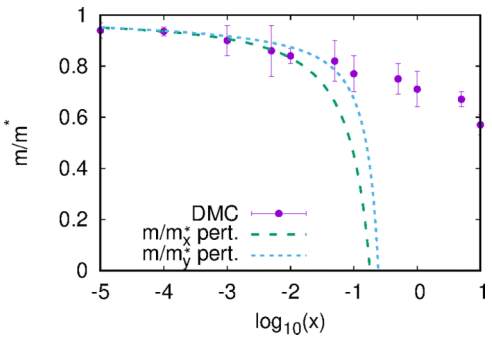

FIG. 7. DMC (dots) and second-order perturbation theory (solid line) results for the inverse effective mass (dimensionless) as a function of the gas parameter for $\alpha = 0.6$ rad, $\beta = 1.42$. DMC results correspond to $m/m_x^* \simeq m/m_y^*$ since, in this regime, the DMC estimations of m_x^* and m_y^* are indistinguishable within statistical noise.

quantity of statistical data, are performed. Regardless, we see agreement between the perturbative and DMC results in the regime where $m_x^* \simeq m_y^*$.

The anisotropic character of the effective mass is more clearly seen when correlations are strong. To showcase that, we show in Fig. 8 the DMC results for m/m_x^* and m/m_y^* as a function of the polarization angle for $\beta = 10$ and two values of the gas parameter $x = 1$ and $x = 100$. We can see that, even away from the regime of validity of perturbation theory ($\beta \gg 1$), anisotropic effects in the effective mass follow the qualitative trends predicted by the perturbative calculation, showing indeed that $m_x^* > m_y^*$.

IV. EXPERIMENTAL VIABILITY

Even though some of the gas parameters considered in this work are too high to be experimentally viable, the universality with respect to the tilting angle in the polaronic properties takes place also at moderately high gas parameters $x \sim 0.01$, which lay within the reach of potential experiments and are above, for instance, of the threshold for which universality is lost for the polaron energy of the two-dimensional Fermi polaron, $x \sim 10^{-5}$ [29]. As an example, let us consider a system of Dy atoms of two-dimensional (2D) density n_{2D} in the x-y plane. In a realistic experiment, atoms which lie within a three-dimensional (3D) setup lay the 2D regime if $L_z < a_{3D}$ [70], with L_z the size of the system along the z axis and a_{3D} the 3D scattering length. In experiments, a_{3D} is of the order of the dipolar length a_{dd}, defined as $a_{dd} = mC_{dd}/(12\pi\hbar^2)$. Consider a 2D gas parameter of $x = 0.01$ with a 2D scattering length of $a_{2D} = 962.6a_0$ (which corresponds to $\alpha = 0.4$ for ^{164}Dy atoms) with a_0 the Bohr radius. Taking $L_z = 0.5a_{dd}$, which guarantees that the 3D system is in the 2D regime since a_{3D} should be of the order of a_{dd} or larger, yields a 3D density of $n_{3D} = 1.1 \times 10^{15}$ cm^{-3}. This density is not far from those present in experiments of dipolar gases [38], meaning that this regime where universality is not expected but is reported in our study could be experimentally probed. Moreover, for this particular case, the presence of three-body losses would not be an issue for the formation of the polaron and the subsequent probing of polaronic properties. According to Ref. [71], the characteristic three-body lifetime can be estimated as $t_3 \sim 1/(L_3 n^2)$, with L_3 the three-body loss coefficient, which for Dy atoms is measured to be $L_3 = 1.33 \times 10^{-41}$ m^6/s [41]. For the 3D density considered, this yields $t_3 \simeq 69.3$ ms. This lifetime is significantly higher than the time it takes for the polaron to be formed, which is of the order of μs in experiments for nondipolar atoms [11] and of the order of 0.1 ms for dipolar ones [26].

V. CONCLUSION AND FUTURE PERSPECTIVES

To summarize, we studied the quasiparticle properties of a dipolar impurity immersed in a dipolar bath in two dimensions, both being subject to an external polarization field that makes all dipole moments point in the same direction. To do that, we used the diffusion Monte Carlo (DMC) method, comparing the results to second-order perturbation theory. We showed that, to a large extent, and for a fixed ratio of the boson-boson and impurity-boson scattering lengths, the polaron energy displays universal behavior with respect to the tilting angle since it is only a function of the density n and the boson-boson a_{BB} (or impurity-boson a_{IB}) scattering length. This is directly induced by the same universal behavior of the pair-distribution function, where the isotropic mode dominates. We also showed that the quasiparticle residue shows also universality with respect to the tilting angle, a result that is recovered through perturbation theory even when anisotropic finite range effects are considered. Finally, we showed that the anisotropy of the dipole-dipole interaction

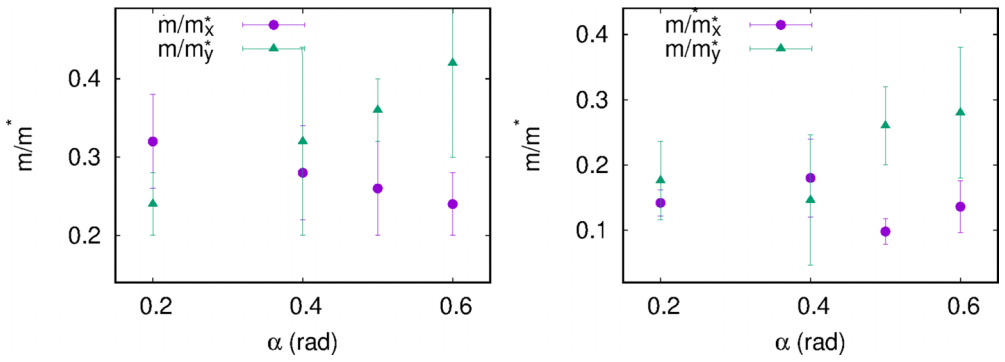

FIG. 8. DMC Results for the inverse effective mass (dimensionless) for (a) $x = 1$ and (b) $x = 100$ as a function of the tilting angle. In both cases, $\beta = 10$.

leads to an anisotropic effective mass which, surprisingly, is larger in the direction of minimum repulsion of the dipole-dipole interaction in position space, which is a consequence of its angular dependence in momentum space. For all the aforementioned properties, we established the regime of validity of perturbation theory in terms of the gas parameter by direct comparison to the DMC results.

Interesting directions for future research include the exploration of the attractive polaron branch and the formation of many-body Efimov states. This is not possible with the interparticle potential employed in the simulations of this work since it lacks any attractive component, but could be done by modeling the interparticle interaction by a dipole-dipole potential plus a short-range repulsive core, and allowing for tilting angles $\alpha > 0.615$ rad. On top of that, the interplay between supersolidity and the polaron could be studied following this same route since this interparticle interaction leads to the formation of a striped dilute liquid [60].

ACKNOWLEDGMENTS

The work was supported by Grant No. PID2020-113565GB-C21 from MCIN/AEI/10.13039/501100011033. L.A.P.A. acknowledges the support of the Deutsche Forschungsgemeinschaft (DFG, German Research Foundation) under Germany's Excellence Strategy–EXC-2123 QuantumFrontiers–390837967, and FOR 2247. L.A.P.A also acknowledges by the PNRR MUR Project No. PE0000023 - NQSTI and the Deutsche Forschungsgemeinschaft (DFG, German Research Foundation) under Germany's Excellence Strategy-EXC-2123 Quantum Frontiers-390837967 and FOR2247

[1] L. Landau and S. Pekar, Zh. Eksp. Teor. Fiz. **18**, 419 (1948).
[2] J. Devreese and F. Peters, *Polarons and Excitons in Polar Semiconductors and Ionic Crystals* (Plenum, New York, 1984).
[3] Z. G, *Polarons in Colossal Magnetoresistive and High-Temperature Superconducting Materials*, Polarons in Advanced Materials, edited by A. S. Alexandrov (Springer Series in Materials Science, New York, 2007), Vol. 103.
[4] C. Hsieh, J. Liu, C. Duan, and J. Cao, J. Phys. Chem. C **123**, 17196 (2019).
[5] C. Kohstall, M. Zaccanti, M. Jag, A. Trenkwalder, P. Massignan, G. M. Bruun, F. Schreck, and R. Grimm, Nature (London) **485**, 615 (2012).
[6] N. B. Jørgensen, L. Wacker, K. T. Skalmstang, M. M. Parish, J. Levinsen, R. S. Christensen, G. M. Bruun, and J. J. Arlt, Phys. Rev. Lett. **117**, 055302 (2016).
[7] M.-G. Hu, M. J. Van de Graaff, D. Kedar, J. P. Corson, E. A. Cornell, and D. S. Jin, Phys. Rev. Lett. **117**, 055301 (2016).
[8] L. A. Peña Ardila, N. B. Jørgensen, T. Pohl, S. Giorgini, G. M. Bruun, and J. J. Arlt, Phys. Rev. A **99**, 063607 (2019).
[9] Z. Z. Yan, Y. Ni, C. Robens, and M. W. Zwierlein, Science **368**, 190 (2020).
[10] J. Etrych, G. Martirosyan, A. Cao, C. J. Ho, Z. Hadzibabic, and C. Eigen, arXiv:2402.14816.
[11] M. G. Skou, T. G. Skov, N. B. Jørgensen, K. K. Nielsen, A. Camacho-Guardian, T. Pohl, G. M. Bruun, and J. J. Arlt, Nat. Phys. **17**, 731 (2021).
[12] H. Cayla, P. Massignan, T. Giamarchi, A. Aspect, C. I. Westbrook, and D. Clément, Phys. Rev. Lett. **130**, 153401 (2023).
[13] N. Darkwah Oppong, L. Riegger, O. Bettermann, M. Höfer, J. Levinsen, M. M. Parish, I. Bloch, and S. Fölling, Phys. Rev. Lett. **122**, 193604 (2019).
[14] E. Braaten, D. Kang, and L. Platter, Phys. Rev. Lett. **104**, 223004 (2010).
[15] W. E. Liu, Z.-Y. Shi, M. M. Parish, and J. Levinsen, Phys. Rev. A **102**, 023304 (2020).
[16] W. E. Liu, Z.-Y. Shi, J. Levinsen, and M. M. Parish, Phys. Rev. Lett. **125**, 065301 (2020).
[17] N. Yegovtsev, P. Massignan, and V. Gurarie, Phys. Rev. A **106**, 033305 (2022).
[18] P. Massignan, N. Yegovtsev, and V. Gurarie, Phys. Rev. Lett. **126**, 123403 (2021).
[19] S. M. Yoshida, S. Endo, J. Levinsen, and M. M. Parish, Phys. Rev. X **8**, 011024 (2018).
[20] N. Yegovtsev and V. Gurarie, arXiv:2305.14638.
[21] L. A. Pena Ardila, G. E. Astrakharchik, and S. Giorgini, Phys. Rev. Res. **2**, 023405 (2020).
[22] N. Yegovtsev, G. E. Astrakharchik, P. Massignan, and V. Gurarie, arXiv:2311.14313.
[23] K. Fujii, M. Hongo, and T. Enss, Phys. Rev. Lett. **129**, 233401 (2022).
[24] E. Nakano, T. Miyakawa, and H. Yabu, arXiv:2404.14866.
[25] A. Tiene, A. T. Bracho, M. M. Parish, J. Levinsen, and F. M. Marchetti, Phys. Rev. A **109**, 033318 (2024).
[26] A. G. Volosniev, G. Bighin, L. Santos, and L. A. P. Ardila, SciPost Phys. **15**, 232 (2023).
[27] K. Nishimura, E. Nakano, K. Iida, H. Tajima, T. Miyakawa, and H. Yabu, Phys. Rev. A **103**, 033324 (2021).
[28] N. Guebli and A. Boudjemâa, J. Phys. B: At. Mol. Opt. Phys. **52**, 185303 (2019).
[29] R. Bombín, T. Comparin, G. Bertaina, F. Mazzanti, S. Giorgini, and J. Boronat, Phys. Rev. A **100**, 023608 (2019).
[30] R. Bombín, V. Cikojević, J. Sánchez-Baena, and J. Boronat, Phys. Rev. A **103**, L041302 (2021).
[31] M. Wenzel, T. Pfau, and I. Ferrier-Barbut, Phys. Scr. **93**, 104004 (2018).
[32] L. A. P. Ardila and T. Pohl, J. Phys. B: At. Mol. Opt. Phys. **52**, 015004 (2019).
[33] B. Kain and H. Y. Ling, Phys. Rev. A **89**, 023612 (2014).
[34] N. Matveeva and S. Giorgini, Phys. Rev. Lett. **111**, 220405 (2013).
[35] A. Camacho-Guardian, Phys. Rev. A **108**, L021303 (2023).
[36] H. Kadau, M. Schmitt, M. Wenzel, C. Wink, T. Maier, I. Ferrier-Barbut, and T. Pfau, Nature (London) **530**, 194 (2016).
[37] M. Schmitt, M. Wenzel, F. Böttcher, I. Ferrier-Barbut, and T. Pfau, Nature (London) **539**, 259 (2016).
[38] I. Ferrier-Barbut, H. Kadau, M. Schmitt, M. Wenzel, and T. Pfau, Phys. Rev. Lett. **116**, 215301 (2016).
[39] L. Chomaz, S. Baier, D. Petter, M. J. Mark, F. Wächtler, L. Santos, and F. Ferlaino, Phys. Rev. X **6**, 041039 (2016).

[40] A. Macia, J. Sánchez-Baena, J. Boronat, and F. Mazzanti, Phys. Rev. Lett. **117**, 205301 (2016).
[41] F. Böttcher, M. Wenzel, J.-N. Schmidt, M. Guo, T. Langen, I. Ferrier-Barbut, T. Pfau, R. Bombín, J. Sánchez-Baena, J. Boronat, and F. Mazzanti, Phys. Rev. Res. **1**, 033088 (2019).
[42] F. Böttcher, J.-N. Schmidt, M. Wenzel, J. Hertkorn, M. Guo, T. Langen, and T. Pfau, Phys. Rev. X **9**, 011051 (2019).
[43] L. Chomaz, D. Petter, P. Ilzhöfer, G. Natale, A. Trautmann, C. Politi, G. Durastante, R. M. W. van Bijnen, A. Patscheider, M. Sohmen, M. J. Mark, and F. Ferlaino, Phys. Rev. X **9**, 021012 (2019).
[44] L. Tanzi, S. M. Roccuzzo, E. Lucioni, F. Famà, A. Fioretti, C. Gabbanini, G. Modugno, A. Recati, and S. Stringari, Nature (London) **574**, 382 (2019).
[45] L. Tanzi, J. G. Maloberti, G. Biagioni, A. Fioretti, C. Gabbanini, and G. Modugno, Science **371**, 1162 (2021).
[46] G. Biagioni, N. Antolini, A. Alaña, M. Modugno, A. Fioretti, C. Gabbanini, L. Tanzi, and G. Modugno, Phys. Rev. X **12**, 021019 (2022).
[47] L. Tanzi, E. Lucioni, F. Famà, J. Catani, A. Fioretti, C. Gabbanini, R. N. Bisset, L. Santos, and G. Modugno, Phys. Rev. Lett. **122**, 130405 (2019).
[48] T. Bland, E. Poli, C. Politi, L. Klaus, M. A. Norcia, F. Ferlaino, L. Santos, and R. N. Bisset, Phys. Rev. Lett. **128**, 195302 (2022).
[49] Y.-C. Zhang, F. Maucher, and T. Pohl, Phys. Rev. Lett. **123**, 015301 (2019).
[50] Y.-C. Zhang, T. Pohl, and F. Maucher, Phys. Rev. A **104**, 013310 (2021).
[51] J. Hertkorn, J.-N. Schmidt, M. Guo, F. Böttcher, K. S. H. Ng, S. D. Graham, P. Uerlings, T. Langen, M. Zwierlein, and T. Pfau, Phys. Rev. Res. **3**, 033125 (2021).
[52] Y.-C. Zhang, T. Pohl, and F. Maucher, Phys. Rev. Res. **6**, 023023 (2024).
[53] J. Sánchez-Baena, R. Bombín, and J. Boronat, arXiv:2312.12164.
[54] A. Macia, F. Mazzanti, and J. Boronat, Eur. Phys. J. **66**, 301 (2012).
[55] A. Macia, J. Boronat, and F. Mazzanti, Phys. Rev. A **90**, 061601(R) (2014).
[56] A. Gallemí and L. Santos, Phys. Rev. A **106**, 063301 (2022).
[57] P. B. Blakie, D. Baillie, L. Chomaz, and F. Ferlaino, Phys. Rev. Res. **2**, 043318 (2020).
[58] J. C. Smith, D. Baillie, and P. B. Blakie, Phys. Rev. A **107**, 033301 (2023).
[59] M. Arazo, A. Gallemí, M. Guilleumas, R. Mayol, and L. Santos, Phys. Rev. Res. **5**, 043038 (2023).
[60] C. Staudinger, D. Hufnagl, F. Mazzanti, and R. E. Zillich, Phys. Rev. A **108**, 033303 (2023).
[61] M. Sohmen, C. Politi, L. Klaus, L. Chomaz, M. J. Mark, M. A. Norcia, and F. Ferlaino, Phys. Rev. Lett. **126**, 233401 (2021).
[62] J. Sánchez-Baena, C. Politi, F. Maucher, F. Ferlaino, and T. Pohl, Nat. Commun. **14**, 1868 (2023).
[63] J. Sánchez-Baena, T. Pohl, and F. Maucher, Phys. Rev. Res. **6**, 023183 (2024).
[64] J. Sánchez-Baena, L. A. P. Ardila, G. Astrakharchik, and F. Mazzanti, SciPost Phys. **13**, 031 (2022).
[65] A. A. T. Durst and M. T. Eiles, arXiv:2404.03980.
[66] A. Macia, F. Mazzanti, J. Boronat, and R. E. Zillich, Phys. Rev. A **84**, 033625 (2011).
[67] S. A. Chin, Phys. Rev. A **42**, 6991 (1990).
[68] A. L. Fetter and J. D. Walecka, *Quantum Theory of Many-Particle Systems* (McGraw-Hill, Boston, 1971).
[69] A. Macia, Microscopic description of two dimensional dipolar quantum gases, Ph.D. thesis, Universitat Politècnica de Catalunya, 2015.
[70] S. Pilati, J. Boronat, J. Casulleras, and S. Giorgini, Phys. Rev. A **71**, 023605 (2005).
[71] M. Krstajić, P. Juhász, J. C. V. Kučera, L. R. Hofer, G. Lamb, A. L. Marchant, and R. P. Smith, Phys. Rev. A **108**, 063301 (2023).